EXPERIMENTAL STUDY AND MODELLING OF THERMAL-DEFORMATION PROCESSES OCCURRING IN WELDED JOINTS ON NICKEL SUPERALLOYS

K.A. YUSHCHENKO[1], **V.A. ROMANOVA**[2], **R.R. BALOKHONOV**[2], **V.S. SAVCHENKO**[1],
N.O. CHERVYAKOV[1] and **A.V. ZVYAGINTSEVA**[1]
[1]E.O. Paton Electric Welding Institute, NASU, Kiev, Ukraine
[2]Institute of Strength Physics and Materials Science, SB RAS, Tomsk, Russia

Results of experimental and numerical investigations of the processes of deformation and fracture of welded joints on nickel superalloys under conditions of mechanical and thermal loading are presented. Structural transformations were investigated, and thermal-deformation processes in the heat-affected zone (HAZ) during the welding cycle process were evaluated. The mechanisms of initiation and propagation of hot cracks in the HAZ metal near the fusion line were determined, and local plastic strains under the thermal cycle condition were assessed. Evolution of the stress-strain state in the HAZ metal was analysed in terms of physical mesomechanics, and conclusions on the role of grain boundaries in the processes of initiation and propagation of cracks were made.

Keywords: *arc welding, nickel superalloys, welded joints, thermal loading, inter-grain boundaries, hot cracks, numerical modelling*

Nickel-base superalloys are characterised by high mechanical properties, but low weldability. They exhibit sensitivity to hot cracking under the welding cycle conditions. Experimental data [1–4] indicate that the thermal cycle of welding leads to substantial structural transformations of material in the HAZ adjoining the fusion line. Mostly hot cracks form in this zone.

To find out causes of hot cracking under the welding cycle conditions it is necessary to have a clear idea of the kinetics of the deformation processes and evolution of the stress-strain state in different zones of a welded joint. So far the information available on these phenomena is scanty, as experimental studies are extremely labour-intensive, and money- and time-consuming.

This article describes experimental and numerical studies of the processes of deformation and fracture of welded joints on nickel alloys under conditions of thermal loading. Structural transformations were investigated, thermal-deformation processes in the HAZ metal during the welding cycle were evaluated, the mechanisms of initiation and propagation of hot cracks under the thermal-force effect conditions were determined, and local plastic strains in the HAZ metal in welding of austenitic nickel alloys were assessed by using experimental methods.

Models of the materials under investigation were developed by allowing for the internal structure, and the deformation processes under the thermal cycling conditions were modelled on the base of the obtained experimental data. Development of the model of a material provides for determination of the explicit temperature dependence of its physical-mechanical properties. At a level of the polycrystalline structure, the sources of the concentration of stresses, initiation of plastic shears and microcracks are grain boundaries.

At the mesoscale level the model described the grained structure in its explicit form, and structural transformations fixed in the HAZ metal during the welding cycle processes were allowed for through phenomenological dependences of mechanical properties upon the temperature. Evolution of the stress-strain state in different regions of HAZ under the heating–cooling thermal cycle conditions was investigated numerically.

Investigation of the deformation processes and peculiarities of structural transformations in the HAZ metal under the welding cycle conditions. Investigations were carried out on nickel alloy IN738LC. As shown experimentally, phase transformations of the $\gamma' + \gamma \rightarrow \gamma \rightarrow \gamma + \gamma'$ type occurs in the HAZ region wherein the propagation of cracks takes place. Precipitation of the fine γ'-phase occurs in the HAZ region adjoining the weld. Size of the γ'-phase particles in the base metal and HAZ is 0.4–0.9 and 0.05–0.15 μm, respectively (Figure 1).
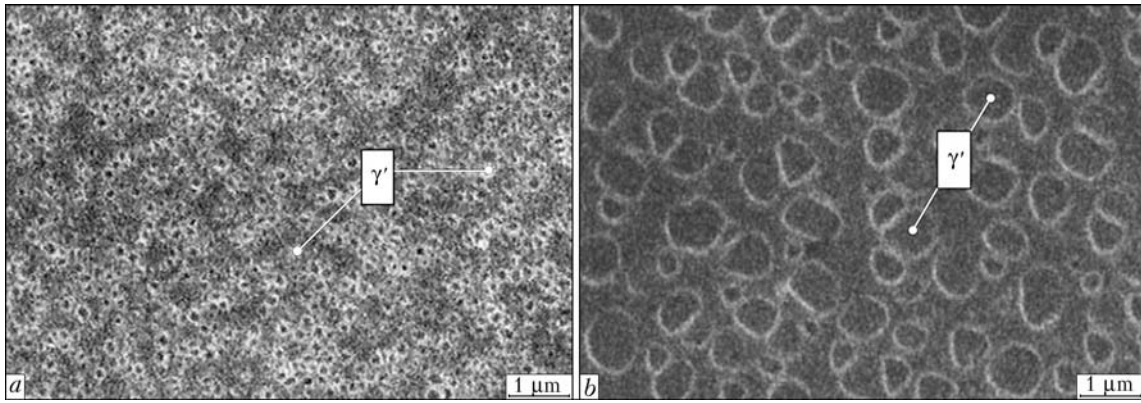
Figure 1. Microstructure with γ'-phase particles in different regions adjoining the weld: a — zone of formation of hot cracks; b — zone of base metal

Temperature of the beginning of dissolution of the γ'-phase particles ($T = 630$ °C) and temperature of complete dissolution of the γ'-phase particles ($T = 1100$ °C) were determined by using the contactless laser dilatometer. It was shown that size of the region where structural transformations take place corresponds to the $T_L - T_{Solv}$ temperature range. Statistical investigations of the presence of defects in welded joints showed that the most probable location of cracks is a zone adjoining the weld. In a general form, the scheme of predominant formation of cracks in the near-weld zone of welded joints on nickel alloys with γ'-strengthening, and its relationship to structural transformations in the HAZ metal, is shown in Figure 2.

Propagation of a formed hot crack along the grain boundaries from zone I (see Figure 2) towards the base metal is inhibited by relaxation of local stresses and plastic strains at the crack mouth (Figure 3, a). It can be seen from the

scheme shown in Figure 3, b that the state of plane deformation takes place in this case. The results obtained are confirmed by optical interference metallography of the surface of the hot crack mouth after welding. It can be seen in Figure 3, c showing the interference pattern, as well as in the region of artificial deformation due to a scratch on the section surface that the course of the interference lines in a region of the crack mouth and scratch tends to move upward. As the scratch is a recess in metal, the zone of metal ahead of the crack shifted downward with respect to the section plane, i.e. shrinkage of metal took place due to realisation of the plastic deformation mechanism.

Analysis of distribution of inter-granular deformation in the welded joint was carried out by
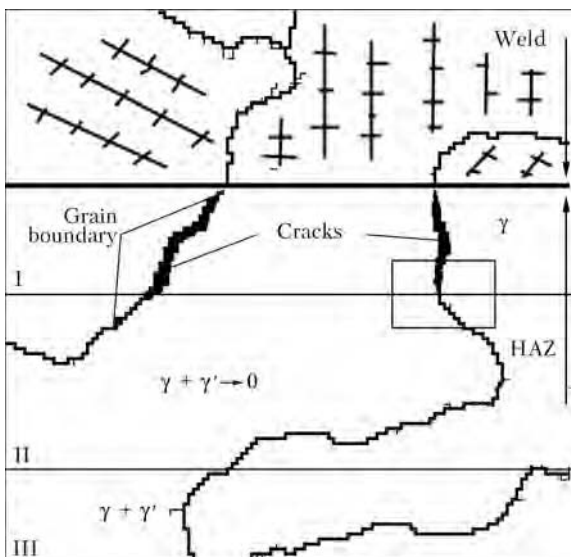
Figure 2. Scheme of predominant formation of cracks in HAZ metal of welded joints on superalloys containing the strengthening γ'-phase: I — zone of complete $\gamma' + \gamma \rightarrow \gamma \rightarrow \gamma + \gamma'$ transformation; II — zone of incomplete transformation; III — zone experiencing no transformations
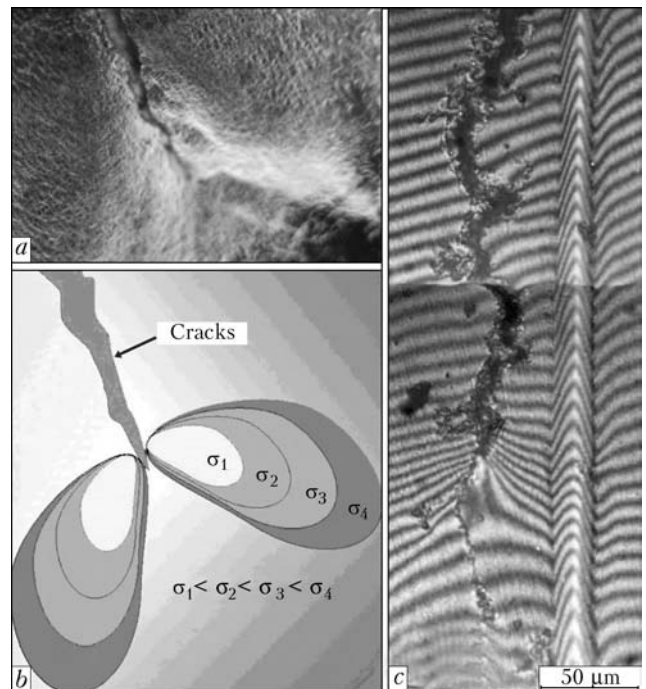
Figure 3. Arresting of hot crack in HAZ metal under the effect of plastic deformation [5]: a — surface of metal at the crack mouth ($\times 400$); b — scheme of distribution of plastic deformation in stress fields; c — plastic strains in the hot crack mouth
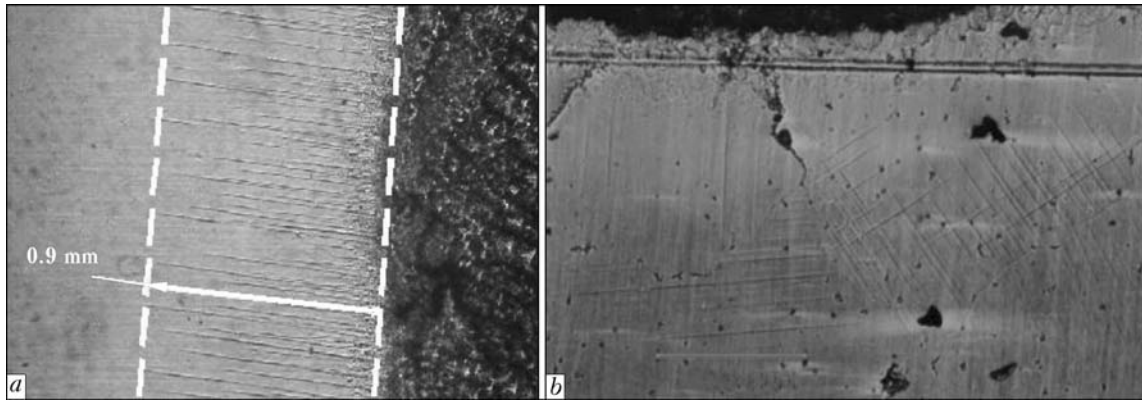
Figure 4. Localisation of plastic strain in HAZ metal near the fusion line (*a*) and development of slip bands inside grains during the welding process (*b* — ×125)

investigation of the geometry of a polished surface of the base metal after welding, the character of fracture of oxide films, as well as the free surface of the electron beam weld metal. Intergranular strains (displacements) in welding are concentrated near the fusion zone, attenuating with distance from it (Figure 4, *a*). The character of inter-granular strains in metal of the near-weld zone depends to a considerable degree upon its phase composition.

Investigations of deformation processes in the HAZ metal on the nickel alloy under the welding cycle conditions were carried out on preliminarily polished plates with a mesh deposited on it. The mesh was made with a diamond tool in the device based on toolmaker's microscope BMI-1, providing thickness of a line equal to 0.01−0.02 mm.

Figure 4, *b* shows a fragment of the surface with slip bands formed in plastic deformation of metal in HAZ, which develops along the slip planes within a grain. The slip system changes in transition to the other grain. Plastic deformation causes orientation rotations in grains.

Numerical investigations of thermal-deformation processes occurring in the HAZ metal were

conducted to understand kinetics of initiation of hot cracks. Nickel alloy (9Cr−9Co−1Mo−10W−6Al−1Ti−2Nb−Ni — base) and stable-austenitic steel (20Cr−16Ni−6Mn−Fe — base) that is insensitive to hot cracking were chosen for comparative calculation analysis.

The thermomechanics problem in the two-dimensional statement was solved numerically by using the finite element method. Detailed formulation of the problem and method used to solve it are presented in [6]. In calculation of elasto-plastic strains and stresses, the experimental data, including elasticity modulus E, yield stress $\sigma_{0.2}$ and linear expansion coefficient α, were determined in a temperature range above 1200 °C. Yield stress $\sigma_{0.2}$ was evaluated by using the ALA-TOO machine IMASH 20-75 (of the «Gleeble» type) in vacuum. Linear expansion coefficient α was determined by the contactless method using the laser beam. Numerical modelling was performed for the case of TIG welding. Sizes of plates and welding heat input in modelling of the thermal-deformation processes were assumed to be the same. Calculation of temperature fields in welding was checked by direct measurements of the thermal cycles in the HAZ metal using thermocouples.

It was found that maximal plastic strains form near the fusion line at a distance of up to 2 mm from it. Dependences of thermal stresses on strains at a point located at a distance of 0.5 mm from the fusion line in welding of the nickel alloy and austenitic steel are shown in Figure 5. At a heating stage (from point 0 to point 2) the material experiences compressive stresses and strains. Point 1 determines the moment of reaching the yield stress value of the material. Point 2 corresponds to the maximal temperature in the thermal cycle and maximal compressive thermal strain. After point 2 there begins the cooling process and, hence, unloading, which continues
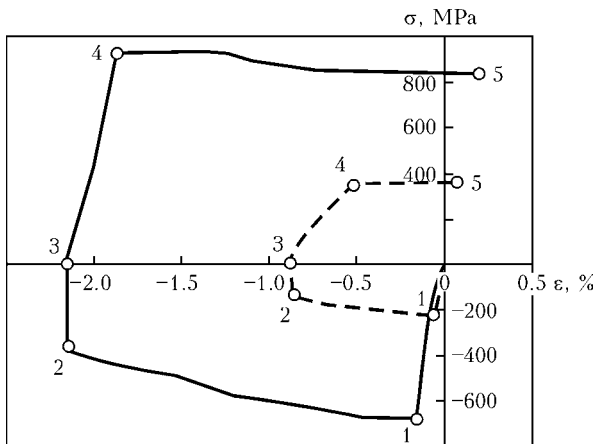
Figure 5. Changes in stresses and strains at a point located at 0.5 mm from the fusion line for nickel alloy (solid line) and for austenitic steel (dashed line): 1−5 — see the text

to point 3, where elastic strains and stresses are equal to zero. Elastic tensile strain grows from point 3 to point 4, and the second plastic strain, but having the opposite sign, starts at point 4. The state at point 5 corresponds to complete cooling of the plate. As shown by calculations, in welding of the nickel alloy at a heat input of more than 350 J/mm, considerable plastic strains (above 3 %) and tensile stresses amounting to yield stress of the material form in the HAZ metal at a distance of up to 2 mm from the fusion line.

Modelling of thermal-deformation processes in the HAZ metal under heating–cooling thermal cycle conditions allowing for the polycrystalline structure. *Mathematical statement of the problem.* In a general case, the stages of modelling include development of a structural-mechanical model of a material, setting of the initial and boundary conditions, and numerical solution of the system of continual mechanics equations allowing for internal interfaces. The general system of the dynamic continual mechanics equations in the Cartesian coordinates system, ignoring the mass forces, includes the following equations:

• equation of motion

$$\rho \dot{U}_i = \sigma_{ij,\,j}; \qquad (1)$$

• equation of continuity

$$\frac{\dot{V}}{V} - U_{i,\,i} = 0; \qquad (2)$$

• energy balance equation

$$\rho \dot{E} = \sigma_{ij}\dot{\varepsilon}_{ij} + \dot{q}^{(e)}; \qquad (3)$$

• relationships for components of tensor of total strain rates

$$\dot{\varepsilon}_{ij} = \frac{1}{2}(U_{i,\,j} + U_{j,\,i}); \qquad (4)$$

• defining relationships that specify connection between components of the stress and strain tensors

$$\sigma_{ij} = f(\varepsilon_{ij}). \qquad (5)$$

Here $U_i = \dot{x}_i$ are the components of the rate vector; x_i are the coordinates; $V = \rho_0/\rho$ is the specific relative volume of the material; ρ_0 and ρ are the initial and current densities, respectively; E is the internal energy; $q^{(e)}$ is the vector of the inflow of heat from external sources; and ε_{ij} are the components of the total strain tensor. The spot under a symbol means the time derivative, and coma after an index — the correspond-

ing coordinate derivative, summation being made on repeating indices i, j, k = 1–3.

It is convenient to present the stress tensor in the form of a sum of the spherical and deviator parts:

$$\sigma_{ij} = -P\delta_{ij} + S_{ij}, \qquad (6)$$

where P is the pressure; S_{ij} are the components of the stress deviator; and δ_{ij} are the Kronecker symbols.

The Duhamel–Neumann equation, which allows for thermal expansion, is used to describe the spherical part of the stress tensor:

$$P = -3K\varepsilon_{kk} + \alpha_t(T - T_0), \qquad (7)$$

where ε_{kk} is the volumetric strain; K is the volumetric compression modulus; α_t is the thermal expansion coefficient; and T_0, T are the initial and final temperatures.

Relationships that connect components of the stress and strain deviator tensors in the elastic loading region are written down in terms of rates in the following form:

$$\dot{S}_{ij} = 2\mu \left(\dot{\varepsilon}_{ij} - \frac{1}{3}\,\delta_{ij}\dot{\varepsilon}_{kk} \right), \qquad (8)$$

where μ is the shear modulus.

Elasto-plastic transition was described by using the Mises yield criterion, according to which the material transforms into a plastic state providing that

$$S_{ij}S_{ij} > \frac{2}{3}\,\sigma_0^2. \qquad (9)$$

In this case, the stress deviator components are reduced to the yield surface through multiplying S_{ij} by the $\dfrac{\sigma_0}{\sqrt{3}\ S_{ij}S_{ij}}$ value, where σ_0 is the yield stress of the material allowing for strain hardening.

The experimental data prove that the elasto-plastic characteristics of nickel-base superaloys demonstrate non-linear dependences on the temperature and size of the γ′-phase. The experimental data for alloy IN738LC [3, 4] were used as a base for determination of approximation dependences for the elasticity modulus and yield stress as functions of temperature, volume content and size of the γ′-phase particles (Figure 6, *b*).

The model sample with a periodic polycrystalline structure (Figure 6, *a*) was generated by the method of stepwise filling [7] on the 100 × × 150 × 100 mesh with a spacing of 2 μm. Periodicity suggests an infinite translation of structure in corresponding directions. For the subsequent solution of the mechanics problem the
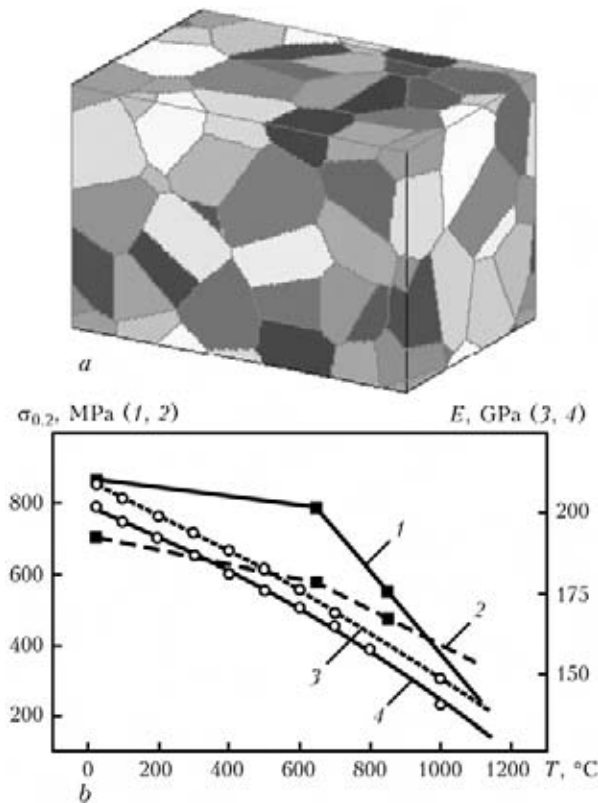
Figure 6. Model polycrystalline structure (*a*) and approximation calculation dependences of mechanical characteristics of alloy IN738LC on temperature and size of the γ'-phase (*b*): *1, 4* — 50—150 nm; *2, 3* — 400—900 nm; points — experiment [3]

periodic boundary conditions can be set on the corresponding surfaces, which are required for more realistic modelling of the restricted deformation conditions.

The effect of crystallographic orientation on the mechanical response of grains was taken into account through scattering of elastic moduli and yield characteristics with respect to the average values within 20 %.

At the same time, mechanical characteristics inside a grain remain constant, although they change in crossing the boundary between the grains.

The equation (1) through (9) system supplemented with the initial and boundary conditions was solved by the numerical finite difference method [8]. The boundary conditions on six surfaces of the calculation sample in the mechanics problem corresponded to the restricted deformation conditions in adiabatic heating. Normal components of the displacement vector on each surface were assumed to be equal to zero. Tangential displacements corresponded to the conditions of absence of the external forces.

Modelling results. According to the experimental data the volume content and size of the γ'-phase particles change during the heating—
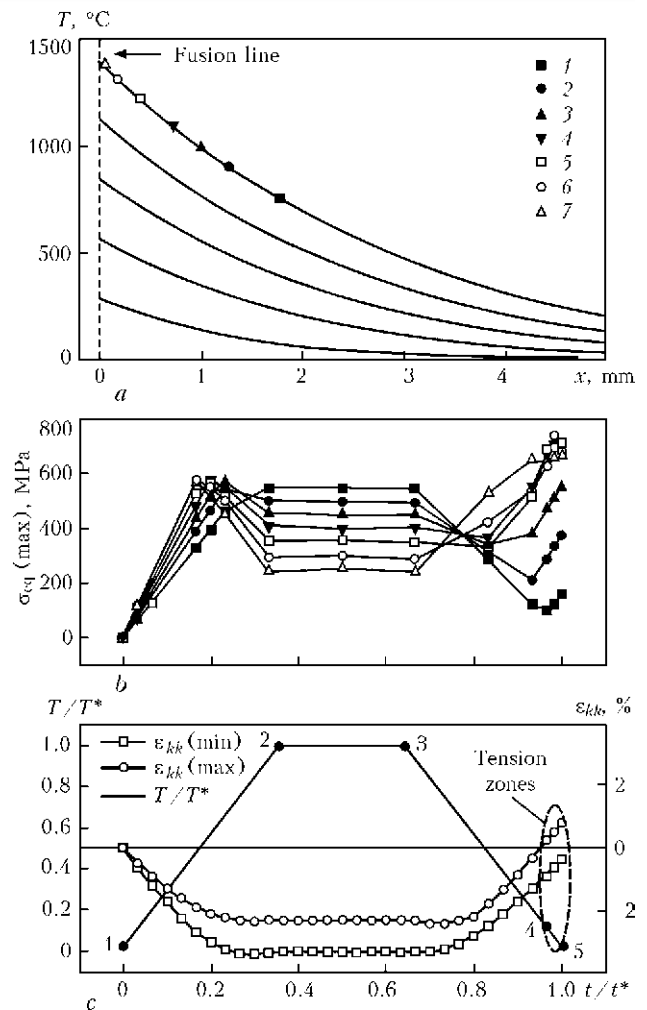
Figure 7. Calculated dependences derived for model polycrystalline grain under the heating—cooling thermal cycle conditions: *a* — distribution of temperature in HAZ metal during heating (*1—7* — regions for which calculations of behaviour of polycrystalline structure were made); *b* — evolution of maximal stress intensity in polycrystalline structure of regions *1—7* at different distances from the fusion line; *c* — variation of temperature and growth of volumetric strain ε_{kk} (*1—5* — see in the text)

cooling thermal process. In the base metal the size of the γ'-phase particles is 0.4—0.9 μm. Dissolution of the γ'-phase begins at a temperature of 630 °C, completely terminating at a temperature of 1100 °C. In cooling the reverse $\gamma \rightarrow \gamma + \gamma'$ transformation takes place. In this case the forming γ'-phase particles are approximately 50—150 nm in size, this causing a change in the mechanical response of the material (Figure 6, *b*). The obtained experimental data were introduced into the model of the mechanical response of grains under thermal loading performed by the heating—cooling scheme shown in Figure 7, *c* on dimensionless coordinates (here T^* and t^* are the maximal temperature of heating and time of the complete cycle, respectively).

Maximal heating temperature T^* was varied in numerical experiments to investigate the
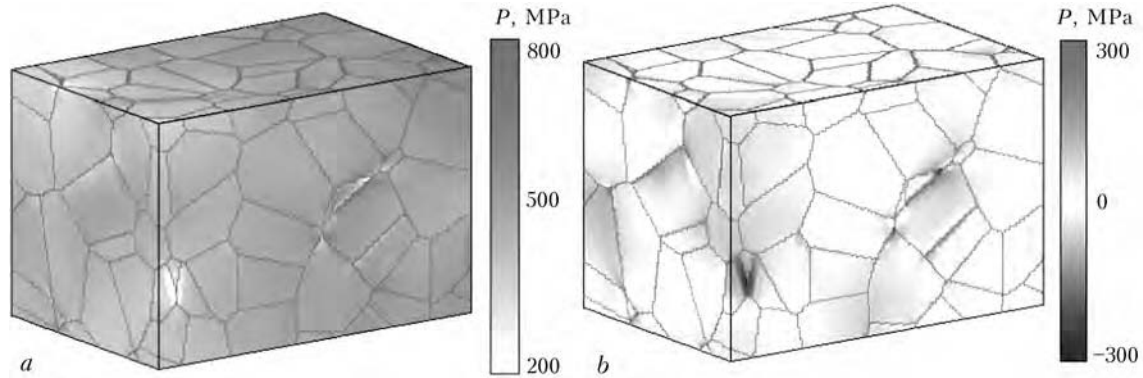
Figure 8. Pressure in HAZ metal at distance of 0.65 mm from the fusion line (T^* = 1100 °C) at points 4 (*a*) and 5 (*b*) of the thermal cycle (see Figure 7, *c*)

stress-strain state occurring at different distances from the fusion line. Variations in temperature through depth of HAZ were determined from the solution of the one-dimensional equation of thermal conductivity

$$\frac{\partial T}{\partial t} = a \frac{\partial^2 T}{\partial x^2}, \quad T(0, t) = f(t), \quad T(L, t) = T_0, \quad (10)$$

where a = 2.6 mm$^2 \cdot$s^{-1} is the thermal diffusivity, and $f(t)$ is the linear function of temperature changing from T_0 = 20 °C to T_{melt} = 1470 °C.

The calculations showed that width of the zone of the complete $\gamma' + \gamma \rightarrow \gamma$ transformation with subsequent precipitation of the fine γ'-phase corresponds to the experimentally determined width of HAZ in welding of the samples with the initial temperature of 20 °C. The maximal temperature gradient within 300 μm (size of the polycrystalline fragment under consideration) was fixed in HAZ near the fusion line, and it was not in excess of 100 °C.

Let us analyse the stress-strain state forming in the polycrystalline structure at a distance of 0.65 mm from the fusion line. Assuming that temperature in the weld zone amounts to melting point T_{melt} = 1470 °C, at a distance of 0.45–0.65 mm from the fusion line the temperature gradient at boundaries of the polycrystalline mesovolume was about 90 °C (see Figure 7, *a*).

Compressive stresses form in the polycrystalline material in the restricted deformation state (Figure 8, *a*) during adiabatic heating (regions 1–2, Figure 7, *c*). Grain boundaries act as sources of a clearly defined concentration of stresses from the very beginning of thermal loading (Figure 9, *a*). The maximal level of stresses is fixed near the triple junction of grains with the most different characteristics. It is here that initiation and propagation of plastic shears take place in subsequent loading (Figure 9, *c*, *d*). The first plastic shears are observed near the fusion line.

More and more distant (from the weld) regions of the HAZ metal are involved into plastic deformation during heating.

At a stage of cooling to room temperature (regions 3–5, Figure 7, *c*) the mean level of stresses falls. However, residual stresses at a distance of 0.65 mm from the fusion line amount to 700 MPa in the local regions of a polycrystalline grain near the grain boundaries that experienced plastic deformation (see Figure 7, *b*).

Modelling of fracture in the problems of mechanics of media with a structure involves certain difficulties, as such a statement imposes extremely high requirements to resolution of the calculation mesh. At the same time, some conclusions on initiation of hot cracks in the HAZ metal can be made on the basis of analysis of evolution of the stress-strain state within the frames of non-equilibrium thermodynamics and physical mesomechanics given in [9, 10]. These studies show experimentally and substantiate theoretically that pores and microcracks in a loaded material initiate in the volumetric tension zones. In this connection, consider now a growth of volumetric strain in the process of the heating–cooling thermal cycle. Figure 7, *c* shows the temperature dependences of growth of maximal and minimal volumetric strains ε_{kk}. Scatter of the relative mean level is caused by a heterogeneous stress-strain state occurring near the grain boundaries. At a stage of heating (regions 1–2, Figure 7, *c*), the volumetric compressive strain grows with growth of temperature, and the scatter related to localisation of strain near the grain boundaries also grows. At a stage of cooling (regions 3–5, Figure 7, *c*), the material tends to return back to the initial state, and volumetric compression decreases. However, the scatter of local strains with respect to the mean level persists, which is associated with development of plastic strain during the previous loading process.
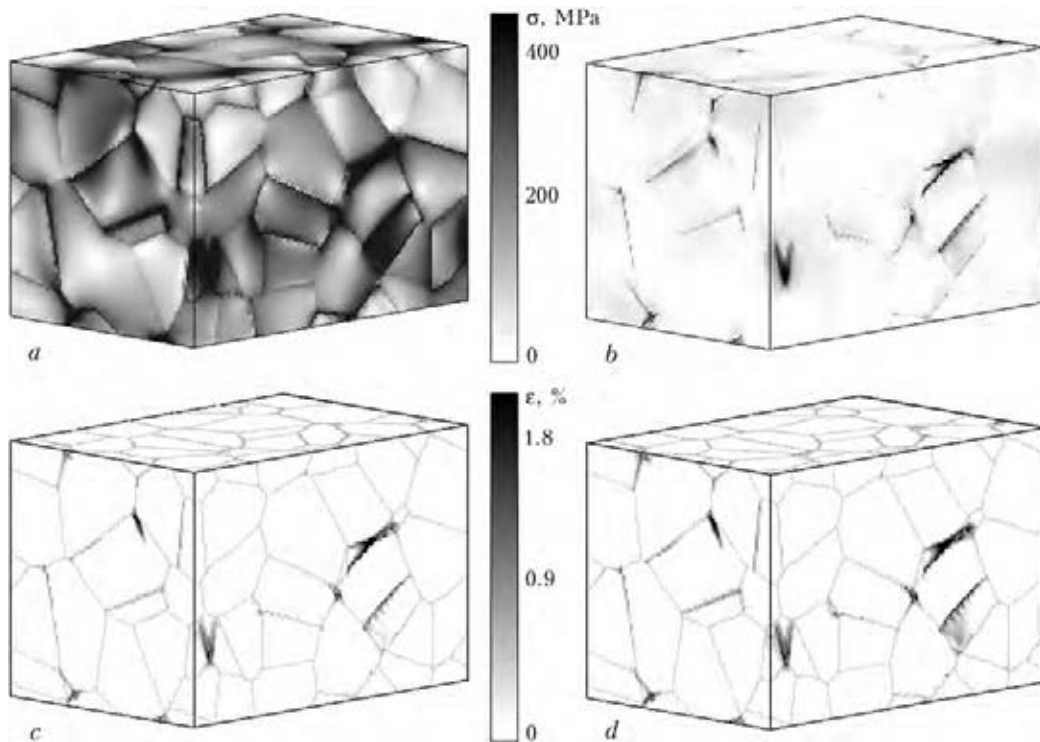
Figure 9. Intensity of stresses (*a*, *b*) and plastic strains (*c*, *d*) in HAZ metal at distance of 0.7 mm from the fusion line ($T^* = 1100$ °C) at points 2 (*a*, *c*) and 5 (*b*, *d*) of the thermal cycle (see Figure 7, *c*)

Finally, at stages 4–5 (Figure 7, *b*), the local volumetric strain propagates into the positive region, which means formation of the local volumetric tension zones (Figure 8, *b*). These zones located near the boundaries of plastically deformed grains (compare Figures 8, *b* and 9, *d*) are potential sources of initiation of hot cracks, providing that the intensity of stresses hear amounts to the tensile strength value. As shown by the calculations made for the polycrystalline grains located in different regions of the HAZ metal, such conditions take place within approximately 0.7 mm from the fusion line.

Evolution of the stress-strain state in the HAZ metal is an extremely complicated process, this being related both to the non-linear dependence of mechanical properties on the temperature, and to the structural transformations near the fusion line.

Analyse now variations in the intensity of stresses in the HAZ metal during the process of the heating–cooling thermal cycle. Curves of the maximal intensity of stresses in different regions of the HAZ metal are shown in Figure 7, *b*. Compare them with variations in temperature during the thermal cycle (see Figure 7, *c*). At the initial stage of heating a linear growth of stresses at a rate corresponding to that of growth of temperature in the corresponding regions of the HAZ metal was fixed in all the HAZ regions considered. A break of all the curves was observed with the beginning of development of plastic shears.

After this break, curves *1–6* in Figure 7, *b* demonstrate a drop of stresses, whereas stresses in a region that is most distant from the fusion line continue growing (curve *7*). This character of evolution of the stress-strain state in different regions of the HAZ metal is determined by two competing processes, i.e. increase in stresses related to further heating, and fall of yield stress in a region of high temperatures. Upon reaching the maximal heating temperature, all the curves go to a stationary level corresponding to region 2–3 (see Figure 7, *c*) of the thermal cycle, after which cooling begins. At the beginning of cooling, the course of the curves is also determined by two competing processes. On the one hand, recovery of yield stress takes place with decrease in temperature, and the material starts showing increase in the compression deformation resistance. On the other hand, there occurs unloading related both to cooling and propagation of plastic shears. Therefore, increase or decrease of local stresses is fixed in different regions of the HAZ metal depending on the distance to the fusion line (compare curves *1–7*, Figure 7, *b*). At the end of the cooling stage all the curves demonstrate a rise related to formation of tensile stresses.

The highest level of residual stresses was fixed near the boundaries of plastically deformed grains within 0.7 mm from the fusion line (curves *4–7*, Figure 7, *b*). These regions are potential zones of development of hot cracks, which then

propagate along the grain boundaries towards the base metal.

CONCLUSIONS

Evolution of the stress-strain state in the HAZ metal of the nickel superalloy under the welding cycle conditions was investigated experimentally and numerically. Special consideration was given to evaluation of local stresses and strains at the mesolevel, where the grain boundaries play an important role. As shown by the experimental and numerical investigations, heterogeneous compressive stresses form at the mesolevel in a polycrystalline structure of the HAZ metal during heating. The sources of a high concentration of stresses are inter-grain boundaries, the maximal level of stresses being fixed at the triple junctions of grains near the fusion line. Plastic shears initiate in these regions. The local zones of volumetric compression, where hot cracks initiate and develop, appear at the cooling stage near the boundaries of plastically deformed grains. Microcracks that initiated at the fusion line propagate along the grain boundaries towards the base metal. The growth of cracks stops at such a distance from the fusion line where the level of local stresses is insufficient to provide their further propagation.

The models considered allow for by no means all the effects related to the most complicated processes occurring under the welding cycle conditions. Fracture in the HAZ metal occurs under conditions of high-temperature creep and under the effect of couple stresses. These processes can be modelled by the excitable cellular automaton method allowing for the forming couple stresses. In this case the flows of local structural transformations along the fusion line in the HAZ metal, as well as along the grain boundaries within the complete $\gamma' + \gamma \to \gamma \to \gamma' + \gamma'$ transformation zone are the driving deformation mechanism. These problems will be considered in the future.

1. Yushchenko, K.A., Savchenko, V.S., Zvyagintseva, A.V. (2004) Effect of heat treatment and degree of alloying on structural changes in nickel alloys. *The Paton Welding J.*, **7**, 12–14.
2. Zvyagintseva, A.V., Yushchenko, K.A., Savchenko, V.S. (2001) Effect of structural changes in high-temperature heating on ductile characteristics of nickel alloys. *Ibid.*, **4**, 13–17.
3. Ibekwe, S.R., Gabb, T. (2005) Impulse excitation study of elasticity of different precipitated microstructures in IN738LC at high temperatures. *J. Materials Eng. and Performance*, **14**, 188–193.
4. Balikci, E., Mirshams, R.A., Raman, A. (2000) Tensile strengthening in the nickel-base superalloy IN738LC. *Ibid.*, 9(**3**), 324–329.
5. Yushchenko, K.A., Savchenko, V.S., Chervyakov, N.O. et al. (2004) Character of formation of hot cracks in welding cast heat-resistant nickel alloys. *The Paton Welding J.*, **8**, 34–38.
6. Makhnenko, V.I. (1976) *Computational methods of study of kinetics of welding stresses and strains.* Kiev: Naukova Dumka.
7. Romanova, V.A., Balokhonov, R.R. (2009) Numerical study of deformation processes on the surface and in the bulk of three-dimensional polycrystalline grains. *Fiz. Mezomekhanika*, 12(**2**), 5–16.
8. Wilkins, M. (1999) *Computer simulation of dynamic phenomena.* Berlin: Springer.
9. Panin, V.E., Egorushkin, V.E. (2009) Physical mesomechanics and non-equilibrium thermodynamics as a methodological basis of nanomaterials science. *Fiz. Mezomekhanika*, 12(**4**), 7–26.
10. Panin, V.E., Egorushkin, V.E., Panin, A.V. (2010) Effect of plastic shear channeling and non-linear waves of localised plastic deformation and fracture. *Ibid.*, 13(**5**), 7–26.